15

Multicharged ion beam release system from the cyclotron

© Y.N. Gavrish, A.V. Galchuck, D.V. Kirzev, Yu.K. Osina, Yu.I. Stogov

JSC „NIIEFA“
196641 St. Petersburg, Russia
e-mail: osina@luts.niiefa.spb.su

Received September 6, 2022
Revised December 23, 2022
Accepted December 24, 2022

NIIEFA have developed and began manufacturing a cyclotron project for the acceleration of multiple-charged ions to energies regulated in the range of 7.5−15 MeV/nucl. The cyclotron electromagnet is H-shaped. The acceleration system consists of two dees, located in „valleys“. Acceleration is performed at even harmonics. Ions are injected from external sources through the axial channel. The classical deflector and magnetic channels extraction system is used.

Keywords: cyclotron, multi-charged ion beam release, mass-to-charge ratio, electrostatic deflector, passive magnetic channel, magnetic channel made of permanent magnets, beam emittance, induction gradient.

DOI: 10.21883/TP.2023.02.55485.217-22

Introduction

Cyclotron of multicharged ions is intended for acceleration of ions with mass-to-charge ratio A/Z = 3−7 (C_{12}^{+3}, O_{16}^{+4}, O_{18}^{+3}, Ne_{20}^{+5}, Si_{28}^{+6}, Ar_{40}^{+10}, Fe_{56}^{+14}, Kr_{84}^{+18}, Ag_{107}^{+22}, Xe_{136}^{+23}, Bi_{209}^{+43}) in the energy range 7.5−15 MeV/nucl. [1]. The multicharged ion (MCI) cyclotron under development will surpass the currently existing DC-280, DC-60, DC-140 ion cyclotrons both in the energy control range and in the range of accelerated ions [2–9]. The closest in characteristics, a wide range of accelerated ions and having the same pole diameter is U-400M cyclotron, the modernization of U-400 cyclotron, created in 1978, and DC-280 cyclotron, put into operation in 2019. (JINR, Dubna) [2,10,11]. However, these cyclotrons fare worse than MCI cyclotron in terms of weight characteristics; besides, the DC-280 cyclotron has a narrower energy control range. The cyclotron of multicharged ions will provide for the first time the acceleration and extraction of bismuth ion beams with high charge from +35 to +43. The variety of ions, the range of changes in their energy and intensity provide the conditions for conducting a wide range of fundamental and applied studies, including for solving a number of technological problems. The development of a complex of multicharged ions, which includes a cyclotron with external injection system, a system for the formation and transportation of accelerated ion beams, a system for irradiating samples and supporting systems, was started in 2020 [1]. The ion flux density range on the irradiated object will be 10^2-10^5 cm$^2\cdot$s^{-1}. Projected beam current from the source for different ions — up to 40 μA. Number of irradiation chambers — 3. In this paper we present the results of simulation of the system for extraction of multicharged ion beam from cyclotron.

The Table shows the results of calculation of the boundary modes of acceleration of the required ions [9]. For light-weight ions it is possible to obtain higher energies $\sim$ 30 MeV/nucl.

It is supposed to extract the beams of accelerated ions from the cyclotron using a deflector and a system of magnetic channels.

The electrostatic deflector with an angular extension of 37° is installed in a „valley“free of dees. The electric field of the deflector deflects the ions, ensuring that the beam exit beyond the pole of the electromagnet. The working potential on the high-voltage plate — up to 100 kV with a gap between the electrodes of about 7 mm. At the maximum potential, the extraction of light-weight ions with increased energy per nucleon is possible.

1. System of magnetic channels of multicharged ion cyclotron

The system of magnetic channels consists of three parts. To correct the gradient of the edge magnetic field on the trajectory of the extracted beam, the first part is used, which serves to focus the beam of accelerated ions deflected by the deflector immediately after the beam exits the sector into the edge field of the cyclotron. The ion beam passing to the regions of the cyclotron edge field sharply decreasing along the radius undergoes defocusing in the horizontal plane and overfocusing in the vertical plane. Without the magnetic channel use it is impossible to obtain reasonable beam sizes at the output flange of the cyclotron in both planes. The first part is fulfilled in the form of two ferromagnetic bars located parallel to the deflected trajectory symmetrically above and below the median plane. The calculated value of the positive radial

Boundary modes of ions acceleration

Element	Charge	Inductance in center, T	Energy, MeV/nucl.
Bi_{209}	35	1.29	7.28
	43	1.6	16.94
Xe_{136}	23	1.29	7.43
	28	1.56	16.12
Ag_{107}	18	1.29	7.35
	21	1.6	15.41
Kr_{84}	14	1.29	7.21
	18	1.5	16.5
Fe_{56}	9	1.41	7.53
	11	1.6	15.44
Ar_{40}	6	1.46	7.5
	10	1.29	16.2
Si_{28}	4	1.5	7.18
	6	1.49	15.93
	9	1.42	32.1
Ne_{20}	3	1.43	7.19
	4	1.56	15.22
	6	1.43	27.9
O_{18}	3	1.33	7.11
	4	1.46	15.44
O_{16}	3	1.29	9
	3	1.6	13
	5	1.42	32.1
C_{12}	2	1.29	7.21
	3	1.29	16.23
	4	1.42	34.4

gradient of the magnetic field introduced by the bars is at least 16 T/m, in the middle zone at the maximum operating mode of the cyclotron (MMF of the main winding 700 kA-turn).

The second and third parts are sets of four permanent magnets forming a quadrupole lens. Required magnetic field induction gradient is ~ 10 T/m.

Electromagnet pole diameter — 4 m [9]. The passive part of the magnetic channel is made of steel 10 and is installed in accordance with the trajectory deflected by the deflector.

The deflected trajectory is the trajectory of a charged particle starting from an equilibrium orbit, for which on the azimuth of the deflector location the weakening of the magnetic field by $\Delta B = (E/0.3) \cdot \beta$ is activated, where ΔB — weakening of the magnetic field, [G]; E — electric field intensity, [kV/cm]; β — particle relative speed.

The trajectory coordinates are computed by integrating the equations of motion of charged particle in the median plane of the calculated magnetic field of the MCI cyclotron.

The magnitude of the electric field strength of the deflector is chosen such that the deflected particle enters the center of the output flange of the cyclotron.

To estimate the magnitude of the magnetic field introduced by the magnetized bars of the 1st part (passive) of the magnetic channels system, a calculation was performed for the minimum and maximum levels of the MMF of the electromagnet of the multicharged ion cyclotron. To compensate for the 1st harmonic from the magnetic field of the steel bars introduced in the beam acceleration region, the second identical pair of bars is installed at an azimuth of 180° from the first. The calculated 3*D*-model of the 1/2 part of the electromagnet with magnetic channel (MCh) and compensator C-MCh1 is shown in Fig. 1.

The vertical section of MCh1 (gradient corrector) showing the boundaries of the magnet pole and sectors, as well as the calculated radial distribution of the magnetic field from the steel bar for the azimuth, on which the bar axis lies at radius of 208 cm, is shown in Fig. 2.

To determine the optimal azimuthal-radial position of the steel bars of the 1st part of the magnetic channel of the MCI cyclotron, a random search method was used to determine the minimum beam size at the entrance to the second part of the magnetic channel (made of permanent magnets) provided that the deflected trajectory enters the center of output flange of the cyclotron. The magnetic field introduced by the bars in this case was synthesized according to the magnitude of the induction of the initial field at the location of the bar axis point on the given azimuth. As a result, the optimal location of the 1st part of the magnetic channel was obtained.

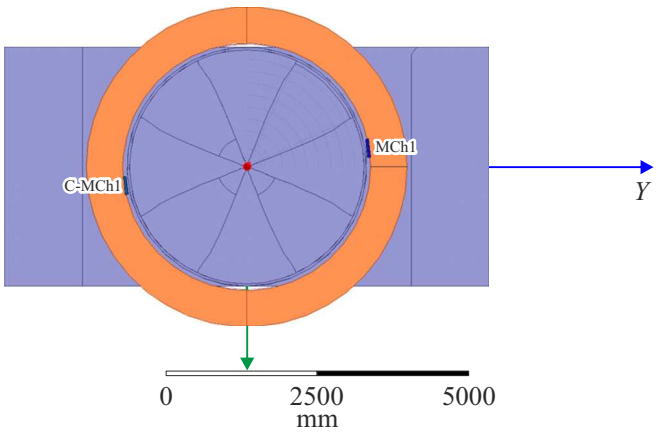

Figure 1. Calculated 3*D*-model of 1/2 part of electromagnet with MCh1 and C-MCh1 compensator, top view.

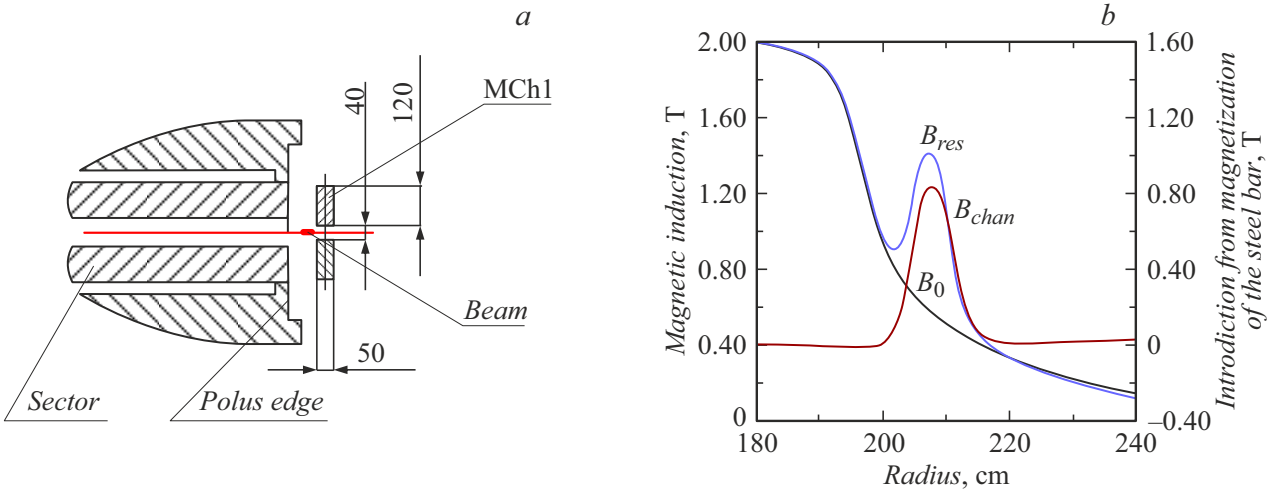

Figure 2. Vertical section of MCh1 showing the boundaries of the pole, sector and beam (*a*) and the radial distribution of the magnetic field from the steel bar for the azimuth at which the axis of the bar lies on radius of 208 cm (*b*); B_0 — magnetic field without bar; B_{res} — magnetic field with inserted bar; B_{chan} — difference in magnetic fields (magnetic field introduced by magnetized bar).

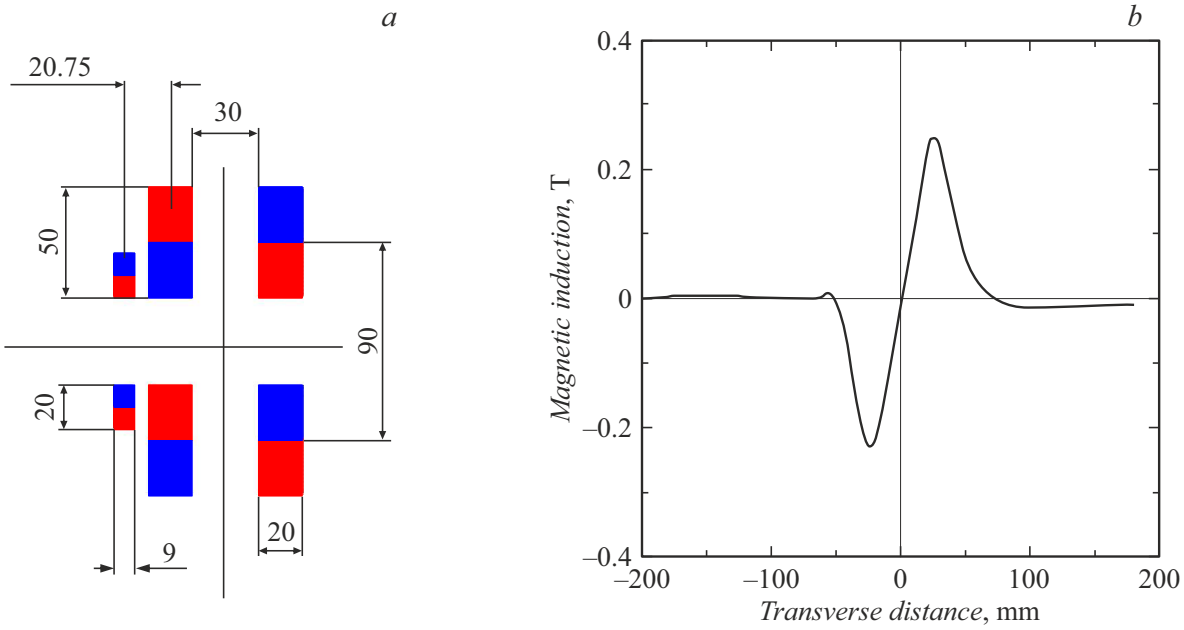

Figure 3. Vertical section of parts 2 and 3 (channels of permanent magnets), the polarity of the magnets is shown for the 2nd part, radially focusing (*a*); distribution of the magnetic field in the median plane along the radius (*b*).

Parts 2 and 3 of the MCh are quadrupole lenses, composed of four permanent magnets, they differ in the order of alternation of the magnets polarity [12]. Material of permanent magnets — Sm_2Co_{17}. Coercive force — 820–860 kA/m.

As a result of numerical simulation, the sizes of permanent magnets providing the gradient ~ 10 T/m are determined. The vertical section of parts 2 and 3 (channels made of permanent magnets) and the magnetic field distribution in the median plane are shown in Fig. 3.

2. Ion beam extraction calculation

Results of calculations for the extraction of beam of Xe_{136}^{+23} ions in magnetic field of 330 kA-turn (7.5 MeV/nucl) and Bi_{209}^{+43} with magnetic channels system in the 700 kA-turn (15 MeV/nucl) mode are presented below. To ensure the beam dimensions within the aperture at the center of the first quadrupole doublet of the MCI cyclotron transportation system, the second and third parts of the MCh were varied in length. The calculations were carried

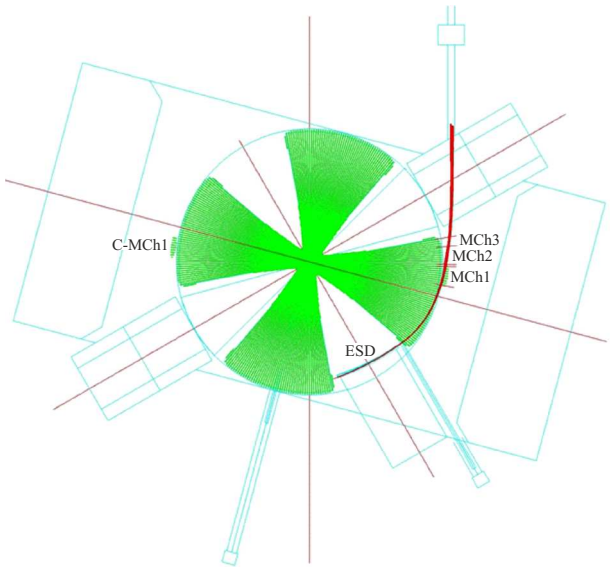

Figure 4. Trajectory of extracted ion beam Xe^{+23}_{136} at ion pipeline of the MCI cyclotron beam transport system in the 330 kA-turn mode (ESD — electrostatic deflector; MCh1 — magnetic channel 1; C-MCh1 — magnetic channel compensator 1; MCh2, MCh3 — radial focusing and vertical focusing magnetic channels made of permanent magnets).

out in the calculated magnetic field with the 1st part of the MCh installed at two levels of the magnetic field — the upper and lower limits of the control range. Since permanent magnets do not affect the field distribution of the main magnet (the material of permanent magnets is characterized by $\mu = 1$), the field from the magnetic channel was simply added to the main field. As the initial conditions at the entrance of the particles beam to the deflector, the maximum oscillation amplitudes were accepted — 5 mm along the vertical and horizontal coordinates, the energy spread is $\pm 0.5\%$. The beam extraction coefficient with the help of deflector is standard, at least 50%.

The calculated trajectory of the deflected beam plotted on the layout plan of the cyclotron is shown in Fig. 4.

The calculated values of the horizontal and vertical emittances of the external beam of Xe^{+23}_{136} ions at the output flange of the MCI cyclotron in magnetic field of 330 kA-turn are shown in Figs 5 and 6.

Similar calculations were also performed for Bi^{+43}_{209} ions for the maximum operating mode of the cyclotron corresponding to 700 kA-turn in the main winding and energy 15 MeV/nucl, respectively. The electric field strength at the deflector during the extraction of Bi^{+43}_{209} ions will be ~ 150 kV/cm. The curves of the deflected beam envelopes, as well as the horizontal and vertical emittances of the external beam of Bi^{+43}_{209} ions at the output flange of the MCI cyclotron in magnetic field of 700 kA-turn, are shown in Figs 7 and 8.

Design documentation for the manufacture of electrostatic deflector and magnetic channel was developed. The design model of the deflector is shown in Fig. 9. The manufacture of the components of the deflector and the magnetic channel continues.

Conclusion

As a result of numerical simulation, the parameters of the devices of the extraction system for the external are

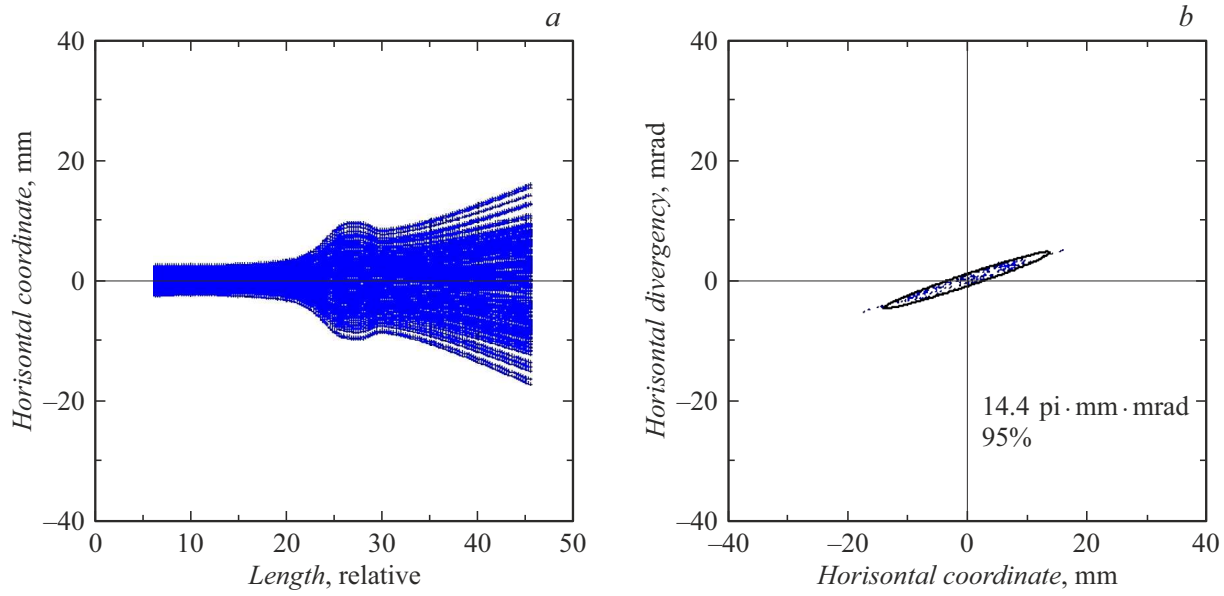

Figure 5. Horizontal envelope of the Xe^{+23}_{136} ion beam from the deflector entrance to the output flange (a) and the beam emittance in the horizontal plane at the cyclotron output flange (b).

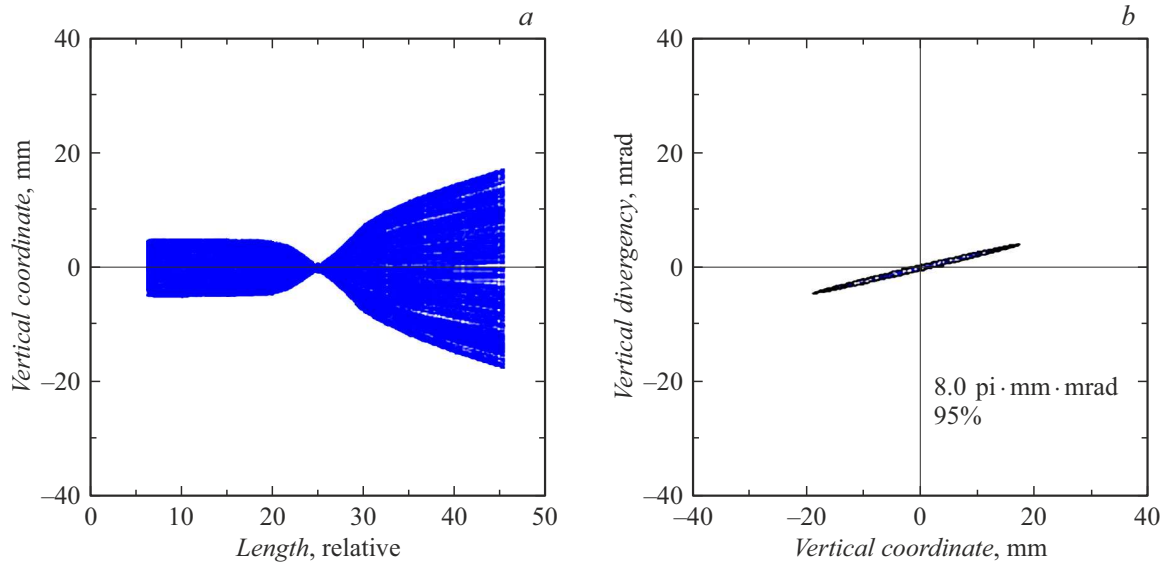

Figure 6. Vertical envelope of the Xe^{+23}_{136} ion beam from the deflector entrance to the output flange (a) and the beam emittance in the vertical plane at the cyclotron output flange (b).

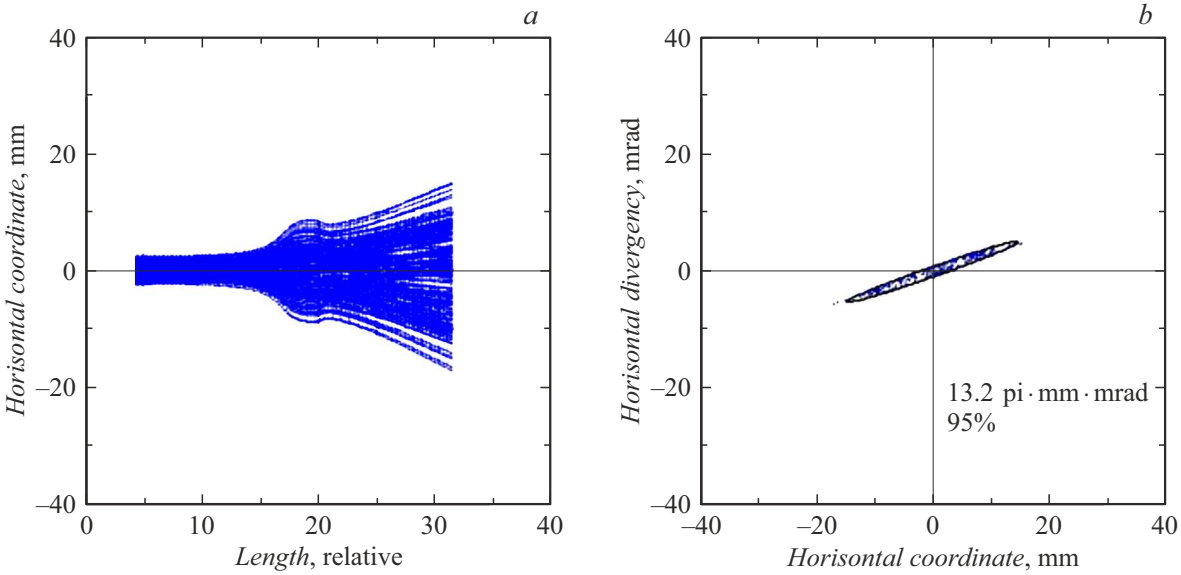

Figure 7. Horizontal envelope of the Bi^{+43}_{209} ion beam from the deflector entrance to the output flange (a) and the beam emittance in the horizontal plane at the cyclotron output flange (b).

determined beam of ions C^{+3}_{12}, O^{+4}_{16}, O^{+3}_{18}, Ne^{+5}_{20}, Si^{+6}_{28}, Ar^{+10}_{40}, Fe^{+14}_{56}, Kr^{+18}_{84}, Ag^{+22}_{107}, Xe^{+23}_{136}, Bi^{+43}_{209} with ratio $A/Z = 3-7$ in the energy control range 7.5–15 MeV/nucl, which will allow minimizing beam losses during the extraction from the cyclotron. The emittance of the beam of Xe^{+23}_{136} ions at the output flange of MCI cyclotron for minimum energy of 7.5 MeV/nucl in the horizontal/vertical plane was $14.4/8\pi \cdot \text{mm} \cdot \text{mrad}$ (95%), of Bi^{+43}_{209} ions for the maximum operating mode of the cyclotron corresponding to the energy 15 MeV/nucl — $13.2/7.3\pi \cdot \text{mm} \cdot \text{mrad}$. MCI cyclotron will provide acceleration of light-weight ions Si^{+9}_{28}, Ne^{+6}_{20}, O^{+5}_{16}, C^{+4}_{12} up to energies ~ 30 MeV/nucl. Thus, the multicharged ions cyclotron being developed by JSC „NIIEFA“ for the first time will provide a wide range of energy control and the extraction of beams of multicharged ions up to bismuth of high charge (+43). The maximum electric field strength on the deflector will not exceed 150 kV/cm.

Currently, work is underway to manufacture all the technological equipment of the multicharged ion cyclotron.

Funding

The work was financed within the under the State Contract with the State Corporation „Rosatom“.

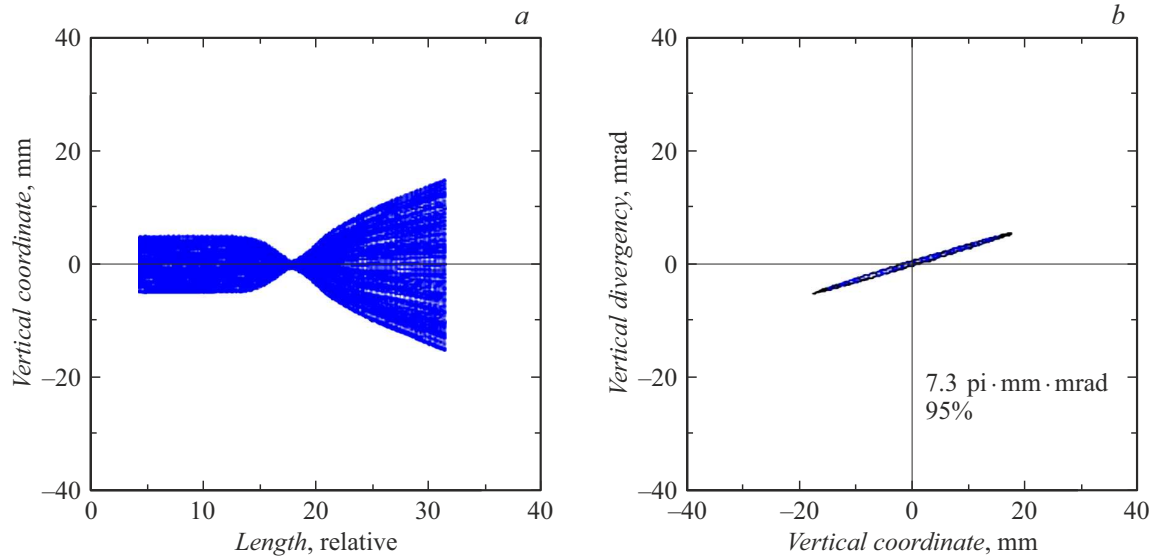

Figure 8. Vertical envelope of the Bi^{+43}_{209} ion beam from the deflector entrance to the output flange (a) and the beam emittance in the vertical plane at the cyclotron output flange (b).

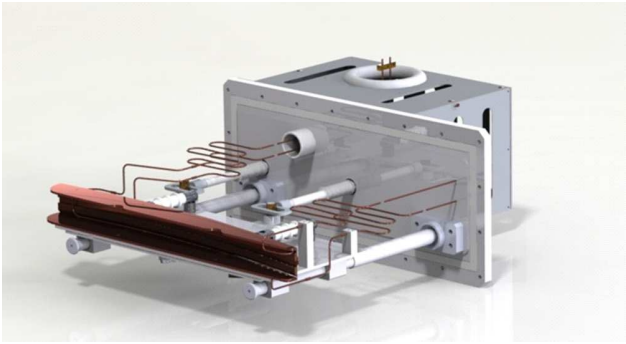

Figure 9. 3*D* deflector model.

Conflict of interest

The authors declare that they have no conflict of interest.

References

[1] Yu.K. Osina, Yu.N. Gavrish, A.V. Galchuk, S.V. Grigorenko, V.I. Grigoriev, R.M. Klopenkov, L.E. Korolev, K.A. Kravchuk, A.N. Kuzhlev, I.I. Mezhov, V.G. Mudrolyubov, K.E. Smirnov, Yu.I. Stogov, M.V. Usanova. Sbornik tezisov dokladov naychno-tekhnicheskoj konferentsii (RFYaTs-VNIITF, Snezhinsk, 15–18 iyunya 2021), s. 5. (in Russian)

[2] G.G. Gulbekyan, S.N. Dmitriev, M.G. Itkis, Yu.Ts. Oganesyan, B.N. Gikal, I.V. Kalagin, V.A. Semin, S.L. Bogomolov, V.A. Buzmakov, I.A. Ivanenko, N.Yu. Kazarinov, N.F. Osipov, S.V. Pashchenko, V.A. Sokolov, N.N. Pchelkin, S.V. Prokhorov, M.V. Khabarov, K.B. Gikal. Pis'ma to EChAYa, **15** (16), 6 (225) (in Russian).

[3] G.G. Gulbekian, S.N. Dmitriev, Yu.Ts. Oganessian, B.N. Gikal, I.V. Kalagin, V.A. Semin, S.L. Bogomolov, I.A. Ivanenko, N.Yu. Kazarinov, G.N. Ivanov, N.F. Osipov. Phys. Particles and Nuclei Lett., **15**, 809 (2018). https://doi.org/10.1134/S1547477118070373

[4] B. Gikal, S. Dmitriev, P. Apel, S. Bogomolov, O. Borisov, V. Buzmakov, G. Gulbekyan, I. Ivanenko, O. Ivanov, M. Itkis, N. Kazarinov, I. Kalagin, I. Kolesov, A. Papash, S. Pashchenko, A. Tikhomirov, M. Khabarov, K. Katyrzhanov, A. Tuleushev, A. Borisenko, S. Lysukhin, V. Aleksandrenko, V. Dektyaryov, V. Dzyubin, M. Koloberdin, K. Kuterbekov, A. Ushakov. Phys. Particles and Nuclei Lett., **5** (7), 642 (2008). DOI: 10.1134/S1547477108070248

[5] B.N. Gikal, G.G. Gulbekyan, O.N. Borisov, A.M. Lomovtsev, V.B. Zarubin, I. A. Ivanenko, N.Yu. Kazarinov, V.I. Kazacha, V.P. Kukhtin, E.V. Lamzin, V.N. Melnikov, S.V. Pashchenko, E.V. Samsonov, O.V. Semchenkova, S.E. Sychevsky, J. Franko. *Formirovanie magnitnogo polya tsiklotrona DC-60* (Preprint OIYaI R9-2006-151), s. 30. (in Russian)

[6] I.A. Ivanenko, G.G. Gulbekyan, N.Yu. Kazarinov, I.V. Kalagin, J. Franko. Pis'ma to EChAYa, **17**(4(229)), 463 (2020). (in Russian)

[7] M. Zdorovets, I. Ivanov, M. Koloberdin, S. Kozin, V. Alexandrenko, E. Sambaev. Proceed. of RuPAC2014, Obninsk, Kaluga Region, Russia, p. 287.

[8] A. Ivanenko, G.G. Gulbekyan, N.Yu. Kazarinov, I.V. Kalagin, J. Franko. Phys. Particles and Nuclei Lett., **17**(4), 473 (2020). DOI:10.1134/S1547477120040202

[9] Yu.K. Osina, A. Akimova, A.V. Galchuck, Yu.N. Gavrish, S.V. Grigorenko, V.I. Grigoriev, M.L. Klopenkov, R.M. Klopenkov, L.E. Korolev, K.A. Kravchuk, A.N. Kuzhlev, I.I. Mezhov, V.G. Mudrolyubov, K.E. Smirnov, Yu.I. Stogov, S.S. Tsygankov, M.V. Usanova.RuPAC2021, Alushta, Russia. 27th Russian Particle Acc. Conf., P. 96. DOI: 10.18429/JACoW-RuPAC2021-FRA02

[10] S. Mitrofanov, B. Gikal, G. Gulbekyan, I. Kalagin, V. Skuratov, Y. Teterev, N. Osipov, S. Paschenko, V. Anashin. Proceedings of RuPAC2014, Obninsk, Russia, p. 152.

[11] B. Gikal, I. Kalagin, G. Gulbekyan, S. Dmitriev. Proceedings of PAC09, Vancouver, BC, Canada FR5REP099, p. 5011.

[12] W. Kleeven, S. Lucas, J.-L. Delvaux, F. Swoboda, S. Zaremba, W. Beeckman, D. Vandeplassche, M. Abs, Y. Jongen. NUKLEONIKA, **48** (Supplement 2), 59 (2003).